

Supplementary Information:

Solvothermal synthesis of metal-organic framework for rapid and selective removal of illegal dyes

Huixiao Duo^{a,b}, Hao Tang^c, Jianlong Ma^{a,b}, Xiaofeng Lu^a, Licheng Wang^{a*},
Xiaojing Liang^{a*}

^aCAS Key Laboratory of Chemistry of Northwestern Plant Resources and Key Laboratory for Natural Medicine of Gansu Province, Lanzhou Institute of Chemical Physics, Chinese Academy of Sciences, Lanzhou 730000, China

^bUniversity of Chinese Academy of Sciences, Beijing 100049, China

^cDepartment of Pharmacy, Gansu Provincial People's Hospital, Lanzhou 730000, China

* Corresponding authors.

Email addresses: wanglc@licp.ac.cn (Licheng Wang); xjliang@licp.ac.cn (Xiaojing Liang)

Phone: +86 931 4968266 Fax: +86 931 8277088

1. Characterization

The powder X-ray diffraction (PXRD) patterns of MOF-235 were obtained with Stoe Stadi-P using Cu K α radiation ($\lambda = 1.54060 \text{ \AA}$) in the range of $5^\circ \leq 2\theta \leq 50^\circ$. The morphologies of the as-prepared materials were characterized by scanning electron microscope (SEM, JSM-6701F, Japan) and BET analyzer (ASAP 2010, Micromeritics, U.S.A). An IFS120HR Fourier transform infrared (FT-IR) spectrometer (Thermo Fisher Scientific, USA) was employed to collect the FTIR spectra with KBr particles at room

temperature. The thermogravimetric analysis (TGA) curves were determined with a thermal gravimetric analyzer (STA449C, Germany) over a temperature range from room temperature to 800 °C at a heating rate of 10 °C·min⁻¹ under an N₂ atmosphere.

2: HPLC conditions

The concentrations of two dyes were determined by an Agilent 1100 Series modular HPLC system (Agilent Technologies, USA) with a high pressure quaternary pump, a 20 μL sample loop and a UV–vis detector. Separation of the analytes was performed on a C18 column (Hypersil ODS2, 250 mm length × 4.6 mm i.d., 5 μm). The mobile phase was methanol and water with 0.2% ammonium acetate. The gradient elution condition was 0–3 min, 15–35% methanol, 3–10 min, 35–80% methanol, 10–12 min, 80% methanol, 12–12.1 min, 80–15% methanol, 12.1–17 min, 15% methanol. Flow rate was set at 1.0 mL/min while the detection wavelength was 500 nm.

3: Chemical structures

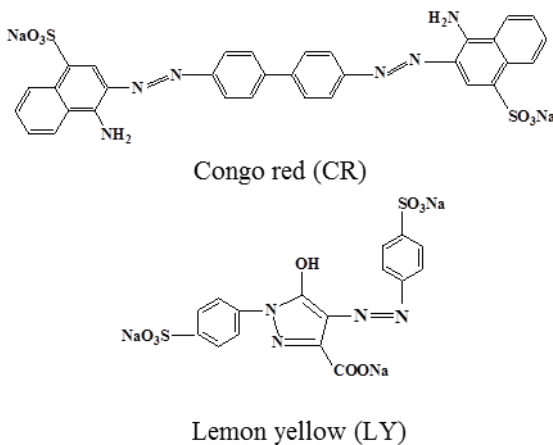


Fig. S1. Chemical structures of two dyes. Congo red (CR) and lemon yellow (LY)

4: Dye adsorption experiment

For equilibrium isotherm, 2 mg of MOF-235 was added to 20 mL glass bottles containing 10 mL of CR solution with initial concentration of 10.0-340.0 mg/L

(pH=3.0) or LY solution with initial concentration of 10-80.0 mg/L (pH=7.0). The resulting mixture was placed into a thermostatic shaker water bath at 25 °C /250 rpm until equilibrium was reached. Thereafter, the solution was centrifuged and analyzed by a HPLC system at the wavelength of 500 nm.

The kinetic experiments for the CR and LY adsorption were carried out by adding 2 mg MOF-235 into 10 mL solution with initial concentration of 240 mg/L (pH=7.0), 80 mg/L (pH=3.0) for CR and LY, respectively. After pretreatment in a thermostatic shaker water bath at 25 °C/250 rpm at a pre-fixed time interval and centrifugal separation process, the concentration in the supernatant, C_t (mg/L), was examined by a HPLC system at the wavelength of 500 nm. The adsorption capacity of CR and LY was calculated by the following equation (2):

$$q_t = \frac{(C_0 - C_t)V}{m} \quad (2)$$

where q_e is the adsorbed amount of dyes per unit mass of the adsorbent (mg/g), C_0 (mg/L) and C_t (mg/L) are the initial and equilibrium concentrations of the dye solution, respectively; V (L) is the initial volume of the dye solution; m (g) is the mass of MOF-235.

5: Characterization of the prepared materials

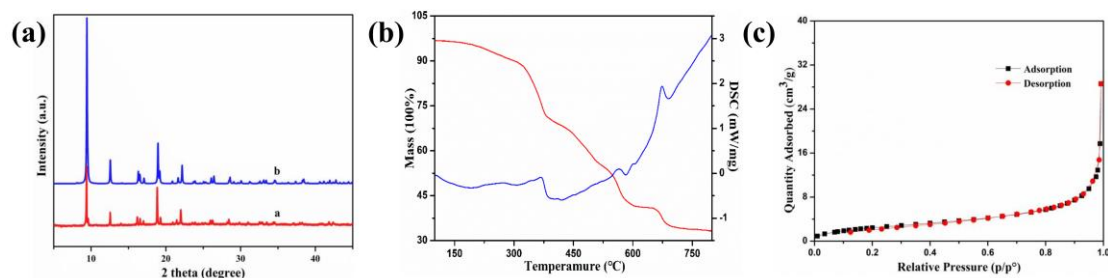


Fig. S2. Characterization of the prepared materials: (a) XRD spectra of as-prepared MOF-235 (a) and MOF-235 (b) in the literature; (b) TGA and DSC curves of MOF-

235 materials; (c) The N₂ adsorption-desorption isotherms of MOF-235.

6: X-ray photoelectron spectroscopy (XPS)

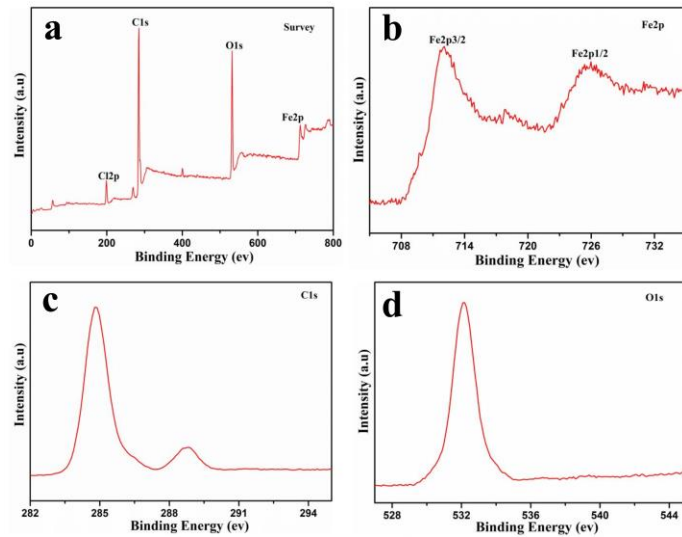


Fig. S3. XPS spectra of the full survey scans of MOF-235 (a) and Fe 2p (b) C 1s (c)

O1s (d) regions corresponding to the spectra of MOF-235.

7: intraparticle diffusion kinetic

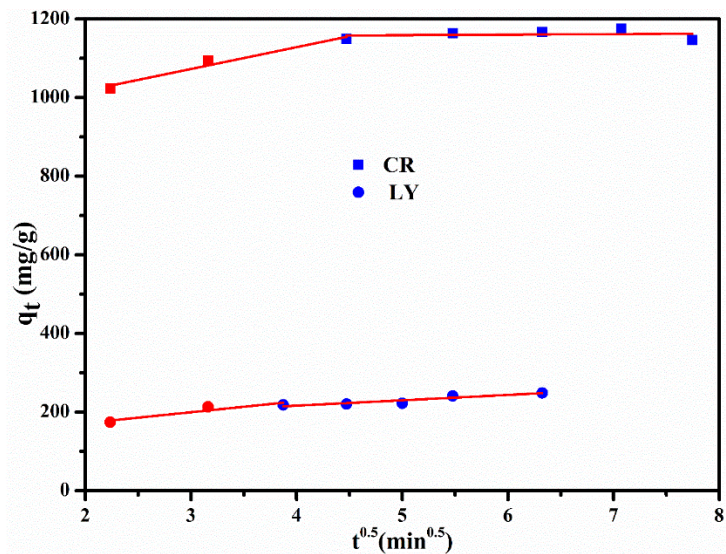


Fig. S4 The linear fitting of intraparticle diffusion kinetic.

8: Regeneration studies

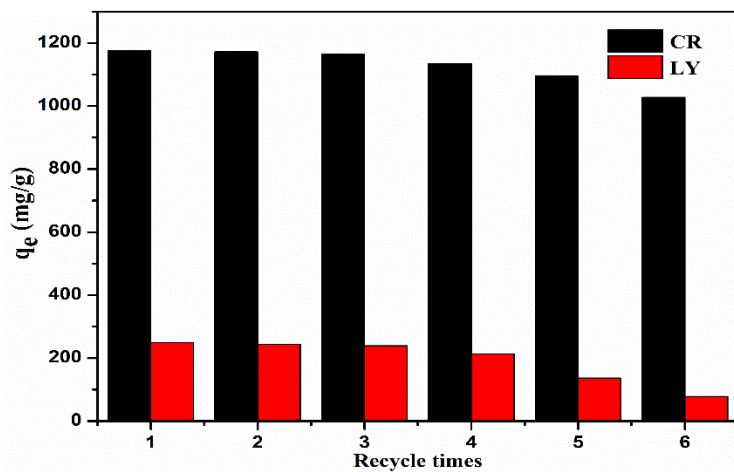


Fig. S5 The reusability of the MOF-235 on adsorption of CR and LY.

9: The BET analysis of reused MOF-235.

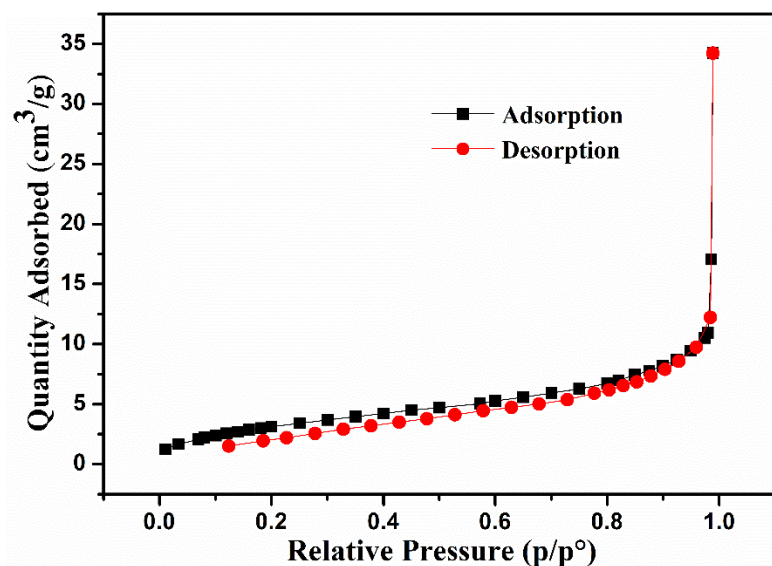


Fig. S6 The N_2 adsorption-desorption isotherms of reused MOF-235.

10: The XRD spectra of reused MOF-235.

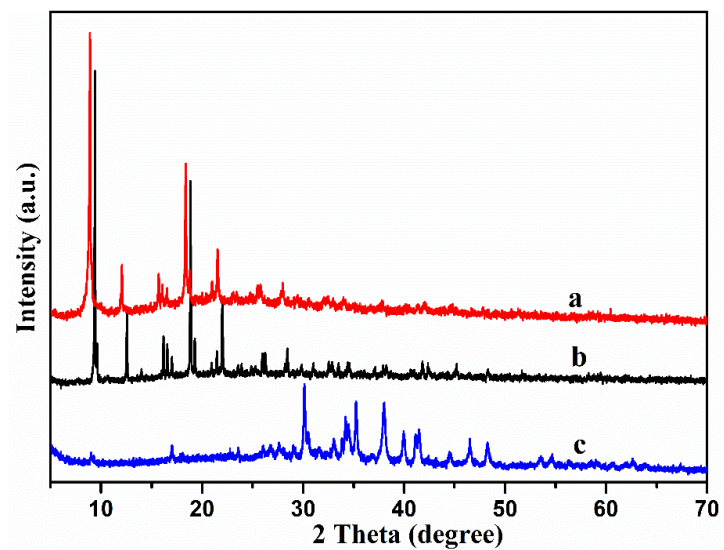


Fig. S7 The XRD spectra of prepared MOF-235 (a), reused MOF-235 (b) and MOF-235 after CR adsorption (c).